Measuring the Effect of ITPP on Tumor Hypoxia with Multispectral Optoacoustic Tomography

Ashley K. Shin[1,2], Caroline E. Robins[2,3], Renee L. Chin[2], Mark D. Pagel[2]

[1]University of Texas Health Science Center at Houston McGovern Medical School, Houston, TX, USA
[2]Department of Cancer Systems Imaging, University of Texas MD Anderson Cancer Center, Houston, TX, USA
[3]Texas Tech University, Lubbock, TX, USA
Author contact information: Ashley Shin; ashley.k.shin@uth.tmc.edu

Introduction:

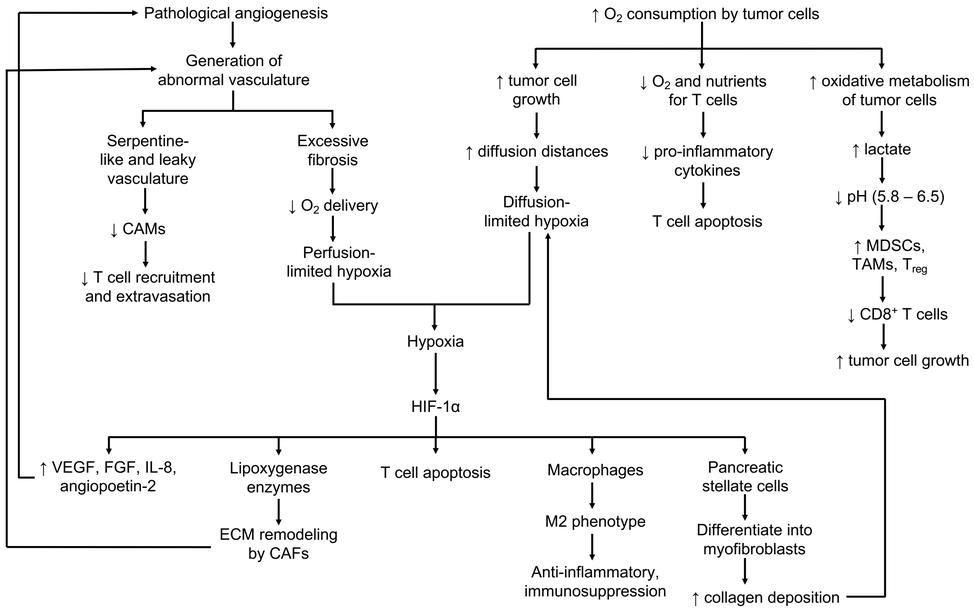

Figure 1: Hypoxia in tumors leads to poor response to T cell-based immunotherapy. A hypoxic tumor microenvironment promotes tumor growth and proliferation. Various factors contribute to hypoxic tumor microenvironment leading to decreased T cell extravasation and increased T cell apoptosis.[1] Abbreviations: CAM, cell adhesion molecules; VEGF, vascular endothelial growth factor; FGF, fibroblast growth factor; IL, interleukin; CAF, cancer-associated fibroblast; HIF-1α, hypoxia-inducible factor 1α; MDSC, myeloid-derived suppressor cell; TAM, tumor-associated macrophage; T_{reg}, regulatory T cell.

Hypoxia within solid tumors creates an environment that promotes tumor growth and development. Hypoxia induces HIF-1α, which increases tumor angiogenesis. Tumor angiogenesis then generates abnormal vasculature leading to decreased expression of vascular adhesion molecules, thus decreasing T cell recruitment and extravasation.[2] Hypoxia also induces an anti-inflammatory, immunosuppressive, M2 phenotype in macrophages that further hinders anti-tumor T cell function and trafficking. In addition, HIF-1α induces T cell apoptosis via Fas to Fas ligand interactions. Because T cells are hindered from entering the tumor environment, the tumors are resistant to T cell-based cancer immunotherapies, thus leading to poor prognoses.[2]

Myo-inositol trispyrophosphate (ITPP) changes oxygen unloading from hemoglobin, thus changes $\%sO_2$.[3] $\%sO_2 = \frac{HbO_2}{Hb+HbO_2}$, where HbO_2 is oxyhemoglobin and Hb is deoxyhemoglobin. ITPP also activates endothelial Phosphatase-and-Tensin-homologue (PTEN), thus inhibiting tumor cell growth and proliferation.[4]

Multi Spectral Optoacoustic Tomography (MSOT) measures deoxyhemoglobin and oxyhemoglobin at distinct wavelengths.[5] MSOT provides a non-invasive way to measure tumor hypoxia to determine response to cancer therapies. Compared to other imaging techniques like magnetic resonance imaging, MSOT is quick, patient-friendly and decreases radiation exposure to patients.

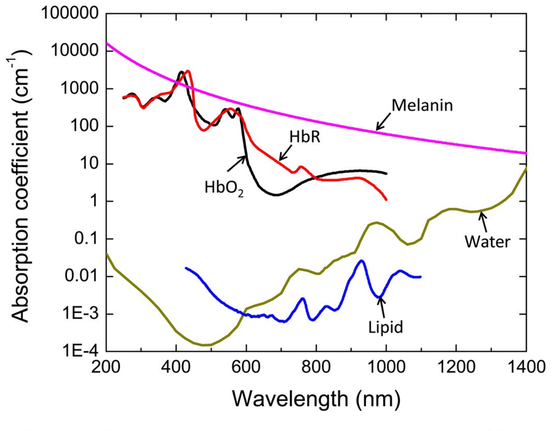

Figure 2: The wavelengths absorbed by various media. MSOT can be used to detect the oxygenation of tumors because oxyhemoglobin (HbO_2) and deoxyhemoglobin (HbR) absorb distinct wavelengths of light. Figure courtesy of iThera Medical, Inc.

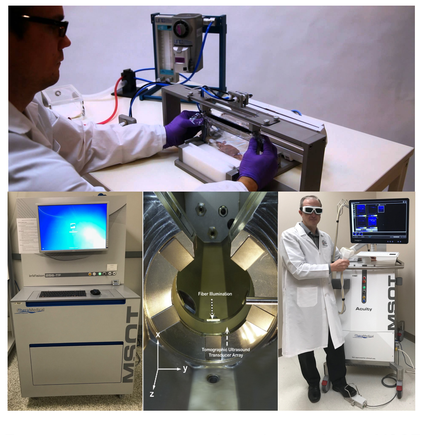

Top: mouse apparatus to be submerged into MSOT machine for imaging; **Lower Left:** MSOT machine for mice and rodents; **Lower Middle:** laser within MSOT; **Lower Right:** clinical MSOT machine

Acknowledgements:

I would personally like to thank Renee Chin, Caroline Robins, Marty Pagel, Michelle Zalles, Jorge de la Cerda, Willian Schuler, and other fellow lab mates for support, assistance with experimentation, and critique. I would like to thank the Small Animal Imaging Facility at the UT MD Anderson Cancer Center. I would also like to express my gratitude for opportunity to be a part of the 2022 MD Anderson Summer Imaging Research Program.

Procedure:

Day 0: Prepare and shave 5 mice (6 weeks of age) around the 4th right inguinal nipple 3 days before implantation
Day 3: Subcutaneous injection of 4T1 tumor cell line mammary epithelial tumor cells into the mammary fat pad
Day 12: Baseline MSOT imaging 9 days post-implantation (tumors are around 4-5 mm in diameter)
Day 13: MSOT imaging 10 days post-implantation and 3 hours post-injection (ITPP or phosphate buffered saline control)

Methods:

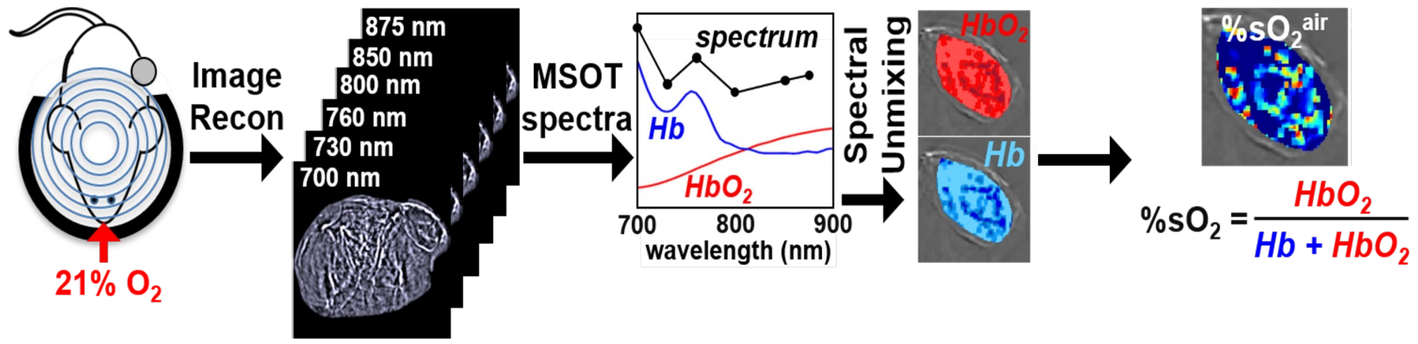

Figure 3: The use of MSOT to determine the level of oxygenation within the tumor environment. Mouse is given 21% medical grade air. MSOT emits light at different wavelengths (700, 730, 760, 800, 850, and 875 nm). The light is absorbed by oxyhemoglobin and deoxyhemoglobin, which undergoes thermoelastic expansion, also known as the optoacoustic effect. The thermoelastic expansion results in ultrasound waves. Images are created from the ultrasound waves. Spectral unmixing of the tumor image separates the oxyhemoglobin and deoxyhemoglobin absorption. $\%sO_2$ is calculated, and the overall oxygenation of the tissue is obtained. The oxygenation levels from the baseline MSOT scan and post-ITPP injection scan are obtained and compared to determine if ITPP improved oxygenation.

Results:

The study of tumor reoxygenation with ITPP as monitored with MSOT is ongoing (Figure 4). As an example of expected results, Figures 5 and 6 demonstrate a related project that shows the classification of normoxic (Su86.86), mildly hypoxic (MIA PaCa-2) and very hypoxic (Colo357) tumors.

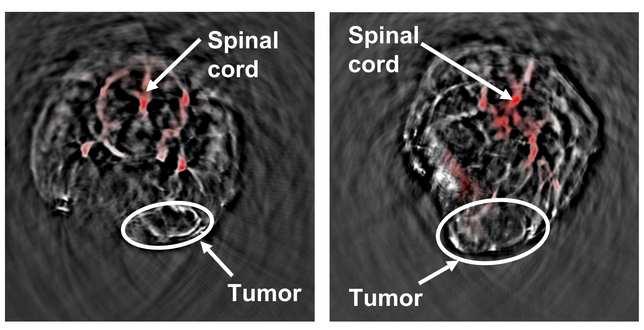

Figure 4: Baseline MSOT image (left) of the 4T1 mammary epithelial tumor on the 4th right inguinal nipple before ITPP injection. **Post-injection MSOT image (right)** of the 4T1 mammary epithelial tumor on the 4th right inguinal nipple 3 hours post-ITPP injection. The tumor was about 4 to 5 millimeters in diameter. The legs and spinal cord were used as landmarks to find the tumor before the scan. After completing the scans, both sets of the tumor scans (baseline and post-injection) were spectrally unmixed to separate the oxyhemoglobin and deoxyhemoglobin absorption.

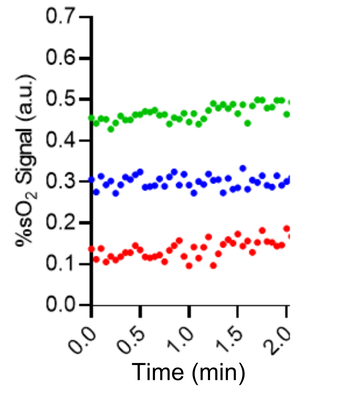

Figure 5: $\%sO_2$ signals from Su86.86 (green), MIA PaCa-2 (blue), and Colo357 (red) tumor models on 21% O_2 medical grade air. At constant temperature. The MSOT showed a consistent measures, confirming the mouse was stable when breathing 21% O_2.

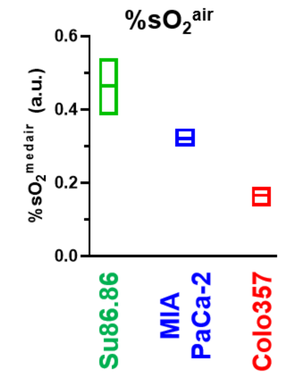

Figure 6: The average value and standard deviation of $\%sO_2$ of 10 mice with Su86.86, 10 mice with MIA PaCa-2, and 10 mice with Colo357, all breathing 21% O_2. Su86.86, MIA PaCa-2, and Colo357 are pancreatic tumor model cell lines obtained from patients and conditioned to grow in immunocompromised mice.

Conclusions:

MSOT has shown to accurately determine the oxygenation of in the Su86.86, MIA PaCa-2, Colo357 pancreatic tumor models in mice. MSOT has the potential to determine changes in tumoral oxygenation in response to ITPP.

Future Directions:

MSOT will continue to be utilized to determine the $\%sO_2$ of tumors. MSOT is currently being tested within the clinical setting on human patients. To continue investigating if ITPP improves the effectiveness of checkpoint blockade, further studies will investigate the effect of ITPP on tumor size and the effect of ITPP on immunogenicity. If ITPP shows to reduce tumor size and increase immunogenicity, the ITPP injection will be effective in improving responses to checkpoint blockade immunotherapy.

Responsible Conduct of Research:

The MD Anderson PI was responsible for maintaining documents and approvals for all modifications in the protocol. All mice were handled in compliance with regulations set by MD Anderson's ethics review board (IACUC).

References:

1. Jayaprakash, P., et al. (2022). Hypoxia reduction sensitizes refractory cancers to immunotherapy. Annual Review of Medicine, 73(1), 251–265.
2. Jayaprakash, P., et al. (2018). Targeted hypoxia reduction restores T cell infiltration and sensitizes prostate cancer to immunotherapy. Journal of Clinical Investigation, 128(11), 5137–5149.
3. Tran, L.-B.-A., et al. (2018). Impact of myo-inositol trispyrophosphate (ITPP) on tumour oxygenation and response to irradiation in rodent tumour models. Journal of Cellular and Molecular Medicine, 23(3), 1908–1916.
4. El Hafny-Rahbi, B., et al. (2021). Tumour angiogenesis normalized by myo-inositol trispyrophosphate alleviates hypoxia in the microenvironment and promotes antitumor immune response. Journal of Cellular and Molecular Medicine, 25(7), 3284–3299.
5. Tomaszewski, M. R., et al. (2018). Oxygen-enhanced and dynamic contrast-enhanced optoacoustic tomography provide surrogate biomarkers of tumor vascular function, hypoxia, and necrosis. Cancer Research, 78(20), 5980–5991.